Modelling and Simulation of a Manipulator with Stable Viscoelastic Grasping Incorporating Friction

A. Khurshid[a], Z. Khan[b], V. Chacko[b], A. Ghafoor[c], M.A. Malik[d], Y. Ayaz[c]

[a] *Department of Mechatronics Engineering, Air University, Sector E-9, Islamabad 44000, Pakistan,*
[b] *NanoCorr, Energy and Modelling (NCEM), Faculty of Science & Technology, Bournemouth University, Dorset BH12 5BB United Kingdom,*
[c] *School of Mechanical and Manufacturing Engineering, National University of Sciences and Technology Sector H-12, Islamabad 44000, Pakistan,*
[d] *Department of Mechanical Engineering, Air University, Sector E-9, Islamabad 44000, Pakistan.*

A B S T R A C T

Design, dynamics and control of a humanoid robotic hand based on anthropological dimensions, with joint friction, is modelled, simulated and analysed in this paper by using computer aided design and multibody dynamic simulation. Combined joint friction model is incorporated in the joints. Experimental values of coefficient of friction of grease lubricated sliding contacts representative of manipulator joints are presented. Human fingers deform to the shape of the grasped object (enveloping grasp) at the area of interaction. A mass-spring-damper model of the grasp is developed. The interaction of the viscoelastic gripper of the arm with objects is analysed by using Bond Graph modelling method. Simulations were conducted for several material parameters. These results of the simulation are then used to develop a prototype of the proposed gripper. Bond graph model is experimentally validated by using the prototype. The gripper is used to successfully transport soft and fragile objects. This paper provides information on optimisation of friction and its inclusion in both dynamic modelling and simulation to enhance mechanical efficiency.

1. INTRODUCTION

Robotic manipulators are usually used for tasks which have been historically performed by human beings by using their hands e.g. in a factory production line. The use of robotic arms is beneficial in several ways as it helps to accomplish repetitive tasks which can cause fatigue in human beings, use of robotic manipulators in hazardous environments reduces risk to human beings (in a paint shop on a factory floor) and exposure to airborne hazardous particles can be avoided. The aim of this research is to develop a humanoid hand with joint friction model and viscoelastic end effectors to provide solutions for performing automated mechanical tasks at maximum performance.

Mechanics of robotic manipulators have been investigated over the past half a century. Mechanics analyses of manipulators have progressed from kinematic to a more complex dynamic analysis over the past two decades. Modelling of complex manipulator linkage mechanisms is now increasingly possible and is being captured more accurately. However, two areas of manipulator mechanisms require further analysis. The first is the dynamic simulation of mechanical manipulators and the effect of joint friction on the dynamics, and the second is, the analysis of interfacial mechanisms between the gripper (manipulator end effector) and corresponding object.

Dynamic simulations have become increasingly popular with increasing computational power and the availability of a wide range of software tools [1]. Several software tools have diverse capabilities in terms of applications. This improves the quality of simulation and reduces the design cycle time. In mechanical systems, the use of a virtual prototype leads to reduction in the overall design cost [2] and virtual prototyping accurately simulates the performance of a system. Visualisation of mathematical models as prototypes in a virtual space provides a better understanding of system performance.

Human fingertips provide soft contact grasping and take on the shape of the object at the interface. Finger deformation at the contact plateaus between 0.2 and 0.9N according to [3] and deformation limit is reached at 1 N. Modified Hertzian contact theory for finger deformation and a power law model has been derived for the deformation of the finger by [4]. Therefore, deformable fingers are superior in comparison to hard grippers and moreover, hard grippers can damage the object. The property of softness also helps in maintaining an increased area of contact during grasping and manipulation which confines the object from moving thus providing a stable grasp [5–9]. Friction at such contact occurs mainly through adhesion [3]. The importance of contact surface engineering has been highlighted in [10] with the introduction of a velvet surface on the gripper. Novel granular material gripper has been presented in [11] which provides an alternative to fingered grasping end effector. Vision based grasping has been presented in [12].

So far several significant contributions have been made in the design of various grippers for grasping and in-grasp fine manipulation [10,11,13–15]. Detailed classification may be found in [16]. Kinematics and dynamics of general robotic manipulators has been presented in [17,18]. A history of robotic arms is given by Monkman [19]. Some of the notable anthropomorphic manipulators are the Salisbury hand (Stanford hand), the Barret hand and the Karlsruhe hand.

The need for task specific robot grippers was addressed through grippers designed to the shape of the workpiece [20]. The same concept has been presented in [13,21]. For use in special environments, the requirement and design of an adaptive finger has been highlighted in [13]. Modification of PUMA robot arm by fitting a humanoid hand with 16 degrees of freedom fingers have been presented in [22].

Postural synergies to control the end effector was presented in [23]. Slip sensing of grasped objects using skin acceleration sensors bonded to silicone skin has been presented by [24]. The application of screw theory for modelling a heavy manipulator has been presented in [25].

Dexterity is the capability of the manipulator to perform certain complex tasks autonomously. Dexterity can be divided into grasping and internal manipulation [16]. However, the dexterity or firmness of grasping is often sacrificed while performing in-grasp fine-manipulation where a pinching grasp is necessary [26]. When holding an object in between fingertips, in-grasp manipulation becomes easy but the chances of slippage and unstable grasp increase at the same time [27]. Therefore, an enveloping grasp is required which is quite dexterous. In-grasp fine manipulation then becomes difficult to achieve. Therefore, the development of such a gripper that makes it possible to provide dexterous grasping and in-grasp fine manipulation simultaneously is a daunting task. Human hand has been analysed from this perspective and the novel 'Huminitive Gripper' is introduced.

The structure of the finger is a key aspect of any anthropomorphic gripper. The finger is made up of flesh with blood vessels inside, and a covering of skin[28]. The fleshy part of the finger imparts

stiffness while the blood inside provides viscous damping. Combination of the two leads to viscoelastic property of fingers. These "soft fingers" deform at contact to take on the shape of the object which ultimately delivers a grasp that is both dexterous and firm. The fingers are visco-elastic and return to their initial shape after the object is released from the grasp. To study the role of stiffness and damping in soft grasping, Bond graph model of soft fingers using a spring-damper combination is developed. Interfacial friction between soft fingertips and the object is incorporated into the contact. This is followed by an analysis of the gripper to evaluate the effects of materials' properties on grasping mechanism within a soft contact.

Table 1. Gripper Classification According to Physical Principle of Operation [19].

Prehension Method	Gripper Type	Typical Examples
Impactive		Clamps (external fingers, internal fingers, chucks, spring clamps), tongs (parallel, shear, angle, radial)
Ingressive	Intrusive	Pins, needles and hackles
	Non- intrusive	Hook and Loop
Astrictive	Vacuum Suction	Vacuum suction cup/bellows
	Magento adhesion	Permanent Magnet/Electromagnet
	Electro adhesion	Electrostatic field
Contigutive	Thermal	Freezing, melting
	Chemical	Permatrack adhesives
	Fluid	Capillary action, surface tension

Table 2. Other Grasping Methods not normally categorized [19].

Gripper	Material Type	Example application
Spoon	Rigid	Loose materials such as nuts and bolts
	Flexible	Powders and viscous fluids
Hook	Rigid	Determinate topology for example castings
	Flexible	Waste material sorting

End effector is the point of interaction with objects in the task environment. Several investigations have been focussed on object manipulation and a fine motion in the past decade [12,29–32]. Tactile [33], visual and grasping controls of multi-fingered robotic hands [23] has been investigated. Research on

material properties and deterioration has been performed by researchers [34–36]. There are two approaches to achieve fine manipulation of the grasped object (i) by manipulating fingers as in a human hand [37–39] or (ii) using the finger tips for fine manipulation of the grasped object [10,26,40,41]. The use of soft fingertips in grasping objects leads to stable grasping [24, 42]. Yet a category for research on a human hand like gripper having soft contact capability and rotating fingers seems to be absent. This has been categorised as "Huminitive Gripper" by [9], and comprises all grippers which resemble and perform soft grasping and fine manipulation like a human hand. The classification of grippers has been explained in [19] (also see Table 1 and Table 2). "*Prehension is the hand's ability to grasp and hold objects of different size and shape, compared to apprehension, which is the hand's ability to understand through active touch*" [16].

The choice of manipulator actuators determines the performance of the manipulators i.e. their dynamics and control. Some of the latest and futuristic actuators have been evaluated. Shape Memory alloys (SMA) deliver large strokes at fast contraction rates and have long life. The analysis of an SMA based miniature manipulator with parallel mechanism has been presented in [43]. SMA's are currently be expensive, prone to hysteresis, require strengthening and have a low energy capacity [44]. Carbon Nano-tubes and polymer fibres have a high work capacity, but need to be redrawn between cycles and were found to be expensive [45]. Work on electro-dynamically driven organic fibres which could render large strokes has been presented in [46]. However, they require special electrolytic envelope, counter electrode, containment systems which make them both heavy and expensive. Pneumatic Air Muscles have been presented in [47,48]. These now have novel pumping mechanism, significant low pressure actuation but can only be actuated linearly with radial expansion. Muscles for controlling the finger are long interwoven and form complex dynamic structures. With several competing technologies showing advancements that address the drawbacks, high performance human muscle substitutes that can be used to activate mechanisms is still closer to reality [46, 49]. Improvements of the hysteresis characteristics of SMA's, the life of CNT wires and decreasing the size of the electrolytic envelope in electrodynamic

fibres will lead to the development of high performance actuators for robotic manipulators in the future. SMA and CNT based actuation seems to be promising for actuators of the future.

This paper has been organised into modelling, simulation and experimentation parts. Mechanical modelling of the manipulator and the gripper are presented in the following section.

2. MODELLING

The kinematics of the manipulator in the Cartesian coordinate system, the dynamics of the arm developed by using the Newton Euler method of formulation, combined joint friction model comprising Coulomb, Viscous and Stribeck friction have been described along with the control of the arm and the development of grasping model using Bond Graph method is presented in the section.

1.1. Kinematics

"*Kinematics pertains to the motion of bodies in a robotic mechanism with no regard to the forces or torques that cause the motion*" [17]. Kinematic model of the arm is made of the geometric relations between links in space and their time derivatives which are; velocity and acceleration. The term Forward Kinematics (FK) usually referring to calculations of end effector position for a given input parameters. Inverse kinematics (IK) on the other hand is referring to joint state parameters calculations from the end effector position. The process of computing IK is complex for higher number of links. Further description of general kinematics may be found in [17]. Here, Denavit-Hartenberg coordinate assignment convention is used [50], [51]. The general kinematic transformation for expressing a point on link i in the coordinate system of the $i-1$ link can be expressed as [50]:

$$p_{i-1} = A_{i-1}^i p_i \qquad (1)$$

$$A_{i-1}^i = \begin{bmatrix} \cos\theta_i & -\cos\alpha_i \sin\theta_i & -\sin\alpha_i \sin\theta_i & a_i \cos\theta_i \\ \sin\theta_i & \cos\alpha_i \cos\theta_i & -\sin\alpha_i \sin\theta_i & a_i \sin\theta_i \\ 0 & \sin\alpha_i & \cos\alpha_i & d_i \\ 0 & 0 & 0 & 1 \end{bmatrix}$$

$$(2)$$

where $i = 1,2,3,4$, A_{i-1}^i is the planar kinematic transformation matrix including rotations and translations. $p_i = \begin{bmatrix} p_{ix} & p_{iy} & p_{iz} & 1 \end{bmatrix}^T$, is the coordinates of the transformation. For this work forward kinematics has been calculated by simulation program and the end effector positions corresponding to input joint angles have been obtained. Dynamic model of the manipulator mechanism is presented in the next section.

1.2. Dynamics

Dynamic model defines the relationship between force and/or torque parameters during the operation of a linkage and/or mechanism. According to Featherstone and Orin, "*The dynamic equations of motion provide the relationships between actuation and contact forces acting on robot mechanisms, and the acceleration and motion trajectories that result*" [18]. Forward dynamics refers to the calculation of the joint trajectories given the actuation forces or torques. Inverse dynamics refers to the calculation of forces and/or torques at joints given the joint positions and its derivatives [18]. Various methods of dynamic modelling have been described in literature: 1) Newton Euler method [52], 2) Euler Lagrange Method [53] and 3) Kane's equation method [54]. The arm may be considered as a constrained multi-link pendulum. Rigid body dynamics equation may be expressed as [52]:

$$D(\theta) + H(\theta,\dot{\theta})\dot{\theta} + G(\theta) + B(\dot{\theta}) = \tau \qquad (3)$$

where θ represents joint angles, $D(\theta)$ represents inertia, $H(\theta,\dot{\theta})$ represents Coriolis and centripetal forces, $G(\theta)$ represents gravity forces, $B(\dot{\theta})$ represents frictional forces, τ represents the joint torques.

Friction is an important phenomenon that affects manipulator motion. It is non-linear and can affect control and positioning of the arm. Therefore, dynamic model of manipulators need to incorporate friction. The practical obstacle is the variation of friction behaviour with the type of joint e.g. anti-friction ball bearings exhibit different behaviour from pin and bush joints. The type of surface finish, lubricant, lubrication condition and the influence of agents determine the friction behaviour of joints [55]. In this work, a friction model composed of Coulomb, viscous

and Stribeck friction is used. Friction values can change due to the influence of environment, as well as wear and tear. τ_{brk} represents the breakaway friction torque which occurs at the start of motion. $\tau_{br.thr}$ represents the threshold breakaway friction torque i.e. the value of torque immediately before the beginning of motion, τ_C represents the Coulomb friction torque, v_{thr} represents the threshold velocity for motion and c_{visc} , c_{trans} represent the coefficients of viscosity and translation respectively. The numerical coefficients have been assumed and have been listed in. The revolute friction model used in the dynamic simulation is represented by the following equations [56]:

$$\tau_f = (\tau_C + (\tau_{brk} - \tau_C).\exp(-c_v|\omega|))\text{sign}(\omega) + f\omega \quad (4)$$

$$\tau_f = \frac{(\tau_C + (\tau_{brk} - \tau_C).\exp(-c_v|\omega_{th}r|))\text{sign}(-c_v\omega_{th}) + f\omega_{thr})}{\omega_{thr}}$$
$$(5)$$

where equation 5 applies in the region of friction transition i.e. $|\omega| < \omega_{thr}$. The value of the parameters is given below in Table 3.

Table 3. Parameters for friction modelling.

Variable Name	Value
τ_{brk}	25 N m
τ_C	20 N m
c_v	0.001 N m s/rad
C_{trans}	10 s/rad
ω_{thr}	1e-4 rad/s
$\tau_{br.thr}$	24.995 N m

The friction model for finger contact is given by [3]:

$$F = \mu N^m \quad (6)$$

Where F is the friction force, μ is the coefficient of friction, N is the normal force and m is an arbitrary constant (≈ 0.3). In this work, friction term in the bond graph model is termed as R_f.

1.3. Control

The developed dynamic model is used for simulation by using a PID controller as shown in **Fig. 1**. The advantage of using a PID controller is the simplicity of design and the ability of the controller to accommodate the temporal variations. The term *P* accounts for the present error values, term *I* includes historical error

values and the *D* value accounts for the future values of error based on the trend. The equation for the PID controller is given by:

$$u(t) = K_p e(t) + K_i \int_0^t e(t)\,\mathrm{d}\,t + K_d \frac{\mathrm{d}\,e(t)}{\mathrm{d}\,t} \quad (7)$$

where K_p is the proportional gain, K_i is the integral gain, and K_d is the derivative gain, *e(t)* is the error in signal between set point value and process variable, t is the time and *u(t)* is the control signal. The tuned parameters for the controller are given as *P* (=144.7), *I* (=2.4), D (=0.01) and N (=2963.35). Results have been presented in Section 4.1.
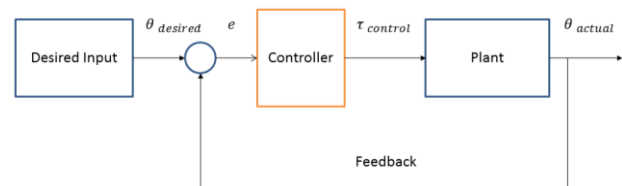

Fig. 1. Schematic of PID Controller.

1.4. Soft contact grasping model

The robotic gripper grasping a cylindrical object has been developed, which has been used to arrive at the required softness to maintain a stable grasp. Fig. **2** shows various cylindrical objects being grasped by using fingers alone. The deformation of the fingers is clearly visible in Fig. 2b.
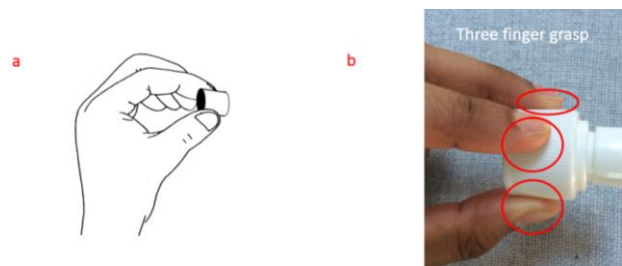

Fig. 2 a. Soft Fingers Grasping a Knob for Fine Manipulation [9], b. Three finger grasp of a cylindrical object.

Three fingers were modelled as soft bodies by using linear mass, spring and damper effects (Fig. 3). Terms Sf1, Sf2 and Sf3 are the forces induced by three fingers for grasping the object. Interfacial friction opposes gravity, preventing the object from slipping through the grasp. The frictional forces are denoted by Rf1, Rf2 and Rf3 at the interface of the gripper and object, the damping coefficients given by Rd1, Rd2 and Rd3. Ks1, Ks2 and Ks3 denotes spring stiffness.
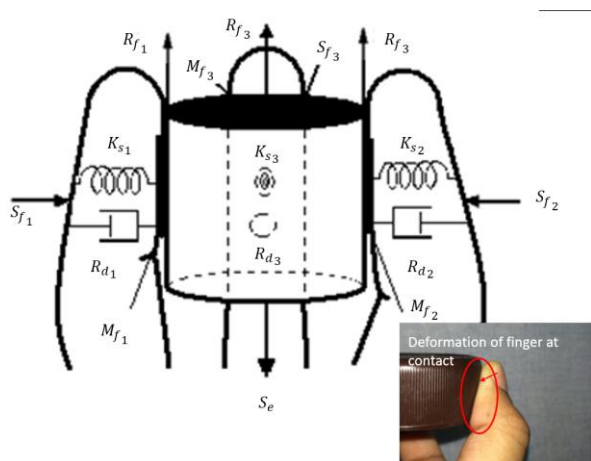
Fig. 3 Schematic diagram of three fingers gripping a cylindrical object with the actual finger deformation (inset).

Fingers' masses are given as Mf1, Mf2 and Mf3. Mo is used to denoted the object mass and Se its weight. Here linear viscoelasticity of soft material has been assumed. Rf, Ks, and Rd were positive time-invariant [41].

1.5. Development of the Virtual Prototype

Computer aided design environment is used to develop a prototype of the arm by using the bottom up approach. Dimensions suitably close to the human arm were assumed for this design and their approximated values have been listed in Table 4.

Table 4. Dimensions suitably approximated values (these can be modified in the future based on anthropometrics).

Part Name	Mass (kg)	Length (mm)
Upper Arm	0.14	118
Lower Arm	0.947	249
Forearm	0.257	423
Hand	0.395	170

Forearm was given a complex form (using loft) to highlight the versatility of the CAD design process. The calculation of link properties such as mass, centre of gravity and moments of inertia are automated in this process. This helps to overcome the tedious calculations for each link for complex designs. Al6061 alloy is used widely in manufacturing robot manipulators for its high its strength to weight ratio and superior machineability and wider

applications [57,58]. Material for the links was then selected to be aluminium alloy material (Al6061). The links were then assembled. The relative link motion is constrained by a one degree of freedom revolute joint between the links (Fig. 4). The simulation of arm dynamics has been explained in the next section.
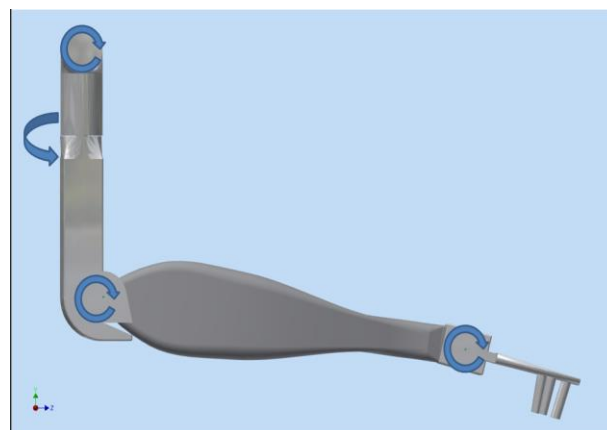

Fig. 4 CAD Design for the humanoid robotic manipulator with single degree of freedom joints.

2. Simulation

2.1. Dynamics of the arm

The novel modelling method considers the concept of frame based physical modelling. The dynamics of the arm have been simulated. The simulations were performed on a workstation powered by a multi-core processor running at 3.20 GHz, with 32 GB RAM running Windows 7 Professional® operating system, equipped with a dedicated Graphics Processing Unit (GPU). The model was developed in the CAD environment and was exported to the multibody dynamics platform.

Fig. **5** shows a graphical layout of the block diagram. The advantage of the method is that links may be iteratively redesigned without having to redesign the whole mechanism. The system also uses physical signals, which can be interfaced with Simulink for control design. In this case, a PID controller has been used to control the plant based on input values. The model is simulated and the controller is tuned to follow the input signal. The results are presented in following sections.
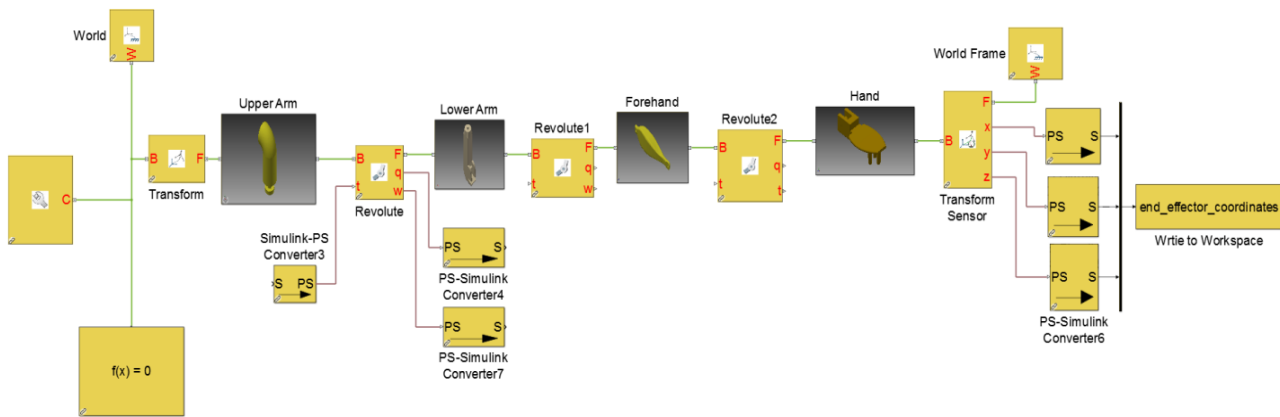
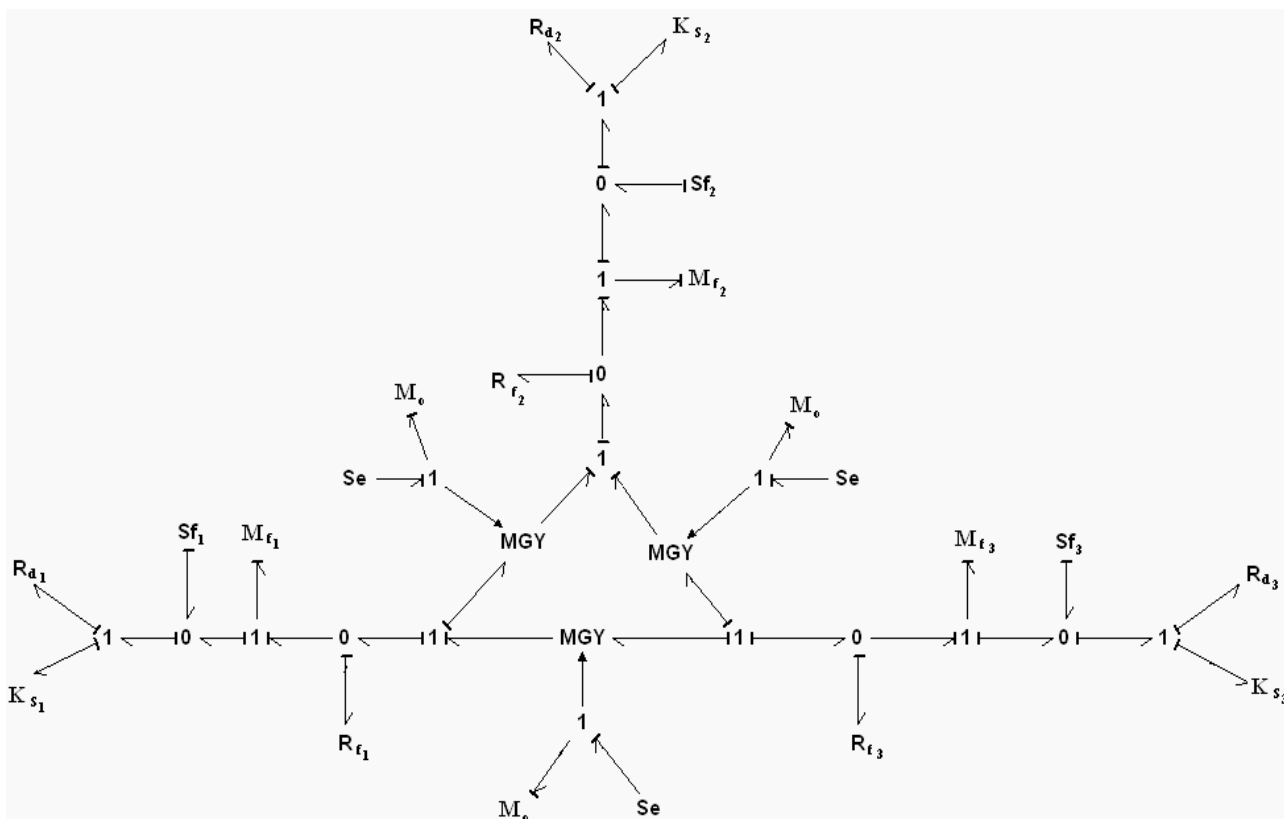**Fig. 5.** Block diagram layout of SimMechanics 2nd generation diagram.

Fig. 6. The contact model of three fingers represented by a Bond graph.

2.2. Bond Graph Model of the hand

The bond graph model for the three-finger gripping contact has been presented in Fig. 6. Application of Bond graph method for various dynamic systems has been discussed in detail by Khurshid et al. [59–61]. Further details of Bond graph construction may be found in [41].

Simulation was performed by using 20Sim. Results from the multi-body dynamics environment and Bond graph simulation have been presented in Section 5.3.

3. EXPERIMENTATION

Two sets of experiments have been presented in this section. The first set measures the friction coefficient through the tribo-testing of steel alloy pair lubricated by grease. The alloy combination is found in pin and bush sliding joints bearings used in manipulator arms. Similar experiments have been reported in [62–64]. The reciprocating mechanism is driven by a scotch yoke mechanism. The displacement is 5 mm and the loading is provided by a cantilevered loading mechanism. The results will provide insight into the performance of grease lubricated contacts

with frequent start stops and conformal contact mechanism. The coefficient of friction was measured for contacts lubricated by commercial off the shelf molybdenum grease. Three load conditions were used for the tests ranging from 25 N to 45 N. The experimental setup for micro-friction tribo-testing is shown in Fig. 7.
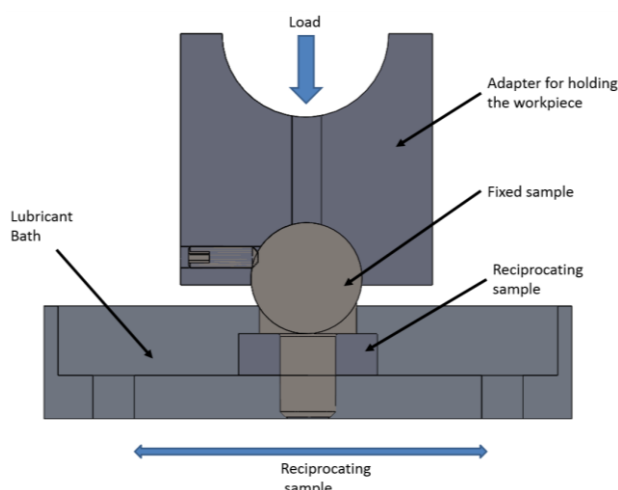

Fig. 7. Experimental setup for micro-friction tribo-testing.

Fig. 8 Process followed by the robotic manipulator in handling the objects.

The second set of results involves the experimental evaluation of the effectiveness of the soft fingertips used to move a soft object and a fragile object between two locations. The process cycle is outlined in
Fig. **8**. The results from the simulations are used to develop an end effector with a viscoelastic interface. The gripper was used to fulfil two tasks successfully. The first task was to pick and place an object which had a smooth exterior and soft composition, i.e. a fruit (tomato) was chosen for its smooth exterior surface and soft body. Fig. **10** shows the grasping, picking and placing of the egg. The second task was performed with a fragile object namely an uncooked egg. The object was picked and placed safely without cracking. The friction parameters for soft finger surfaces have been calculated from the simulations. Both objects remained intact during the experiments because of the soft material (having viscoelastic property) beneath the surface of the fingers [41].

The developed gripper design has been designed for light objects with soft contact with viscoelastic material at tips. Like human fingers, the soft fingertips change their shape to the object being grasped. Planetary gears mechanisms in two of the fingers enable them to provide in-grasp manipulation. This gives the gripper the ability to grasp objects having complex shapes. When the egg was gripped, picked and placed from one place to the other, there was no slippage found practically because of the friction between the egg and soft finger tips was greater than that with the tomato due to the rough surface of the egg. Similarly, no slippage was observed when the tomato is gripped as well. This is because the object is soft and the surface area between the soft finger tips and the tomato surface increases. The results have shown successful gripping without slippage.
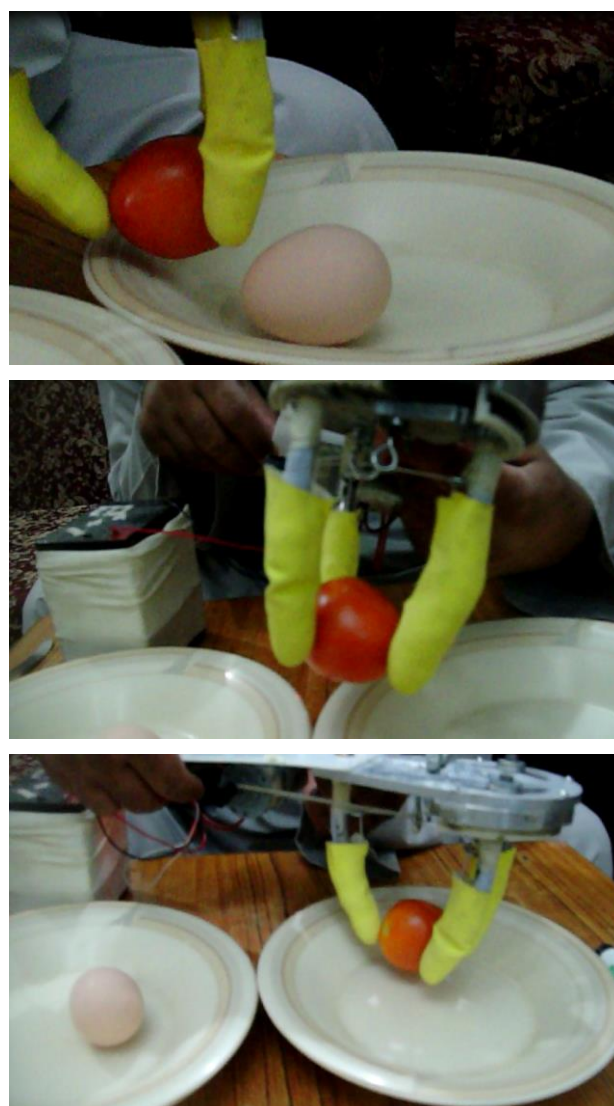
Fig. 9. Gripper having three soft fingers. Grasping, picking, and placing of the tomato have been demonstrated.
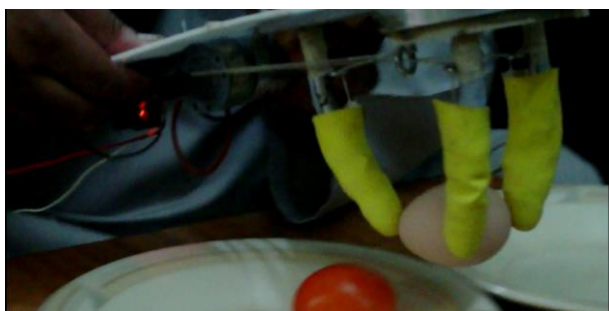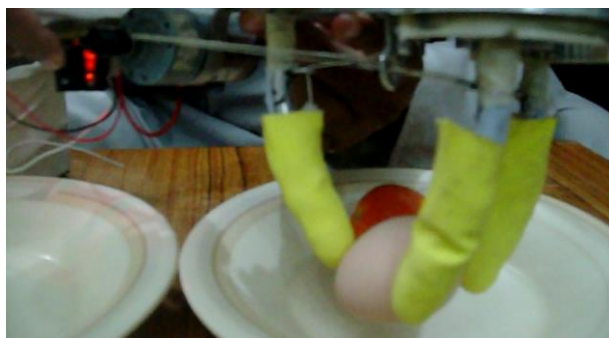

Fig. 10. Experiments with the developed gripper having three soft fingers. Grasping, picking and placing of the raw egg are demonstrated.

4. RESULTS AND DISCUSSION

4.1. Dynamic Simulation

The results of the dynamic simulation of the arm have been presented below. The reach of the manipulator or the extent it traverses the workspace has been illustrated in Fig. 11. Execution times for the different solvers vary. ODE15s solver takes most execution time followed by ODE23s, ODE23tb and ODE23t. ODE15s is suitable for solving stiff differential equations and differential algebraic equations (DAE). Friction torque generated at the joints is presented in Fig. 12. A PID controller has been used to generate control torque which is shown in Fig. 13. Friction torques have been generated

based on the equations (4-7) and presented. Comparison of the end effector motions for different solvers has been presented in
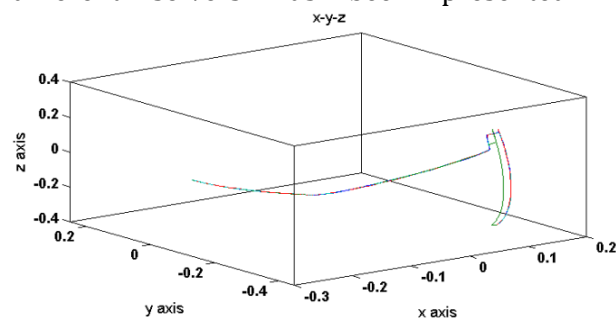

Fig. **14**. Simulations of complex systems require verification and this has been achieved through the comparison of the results.
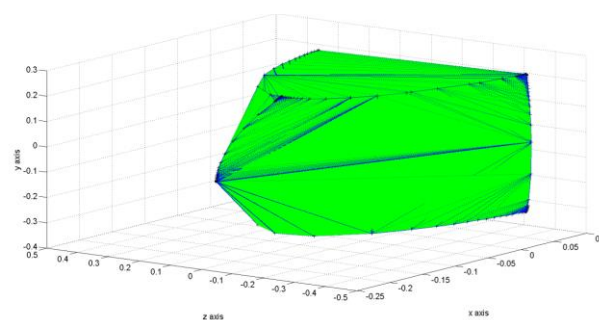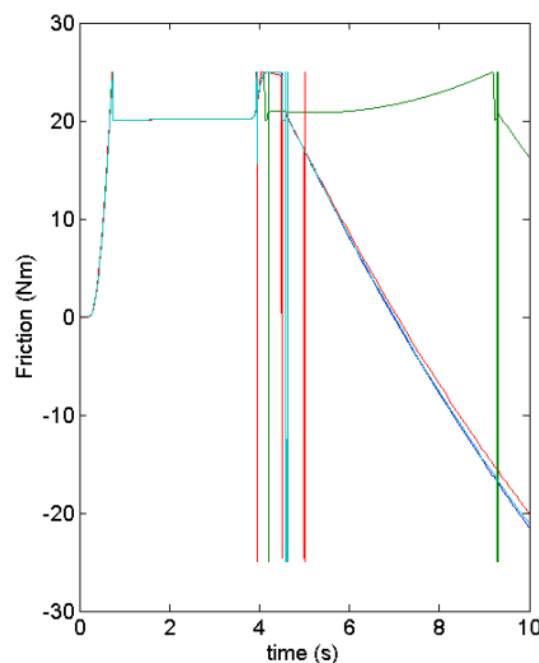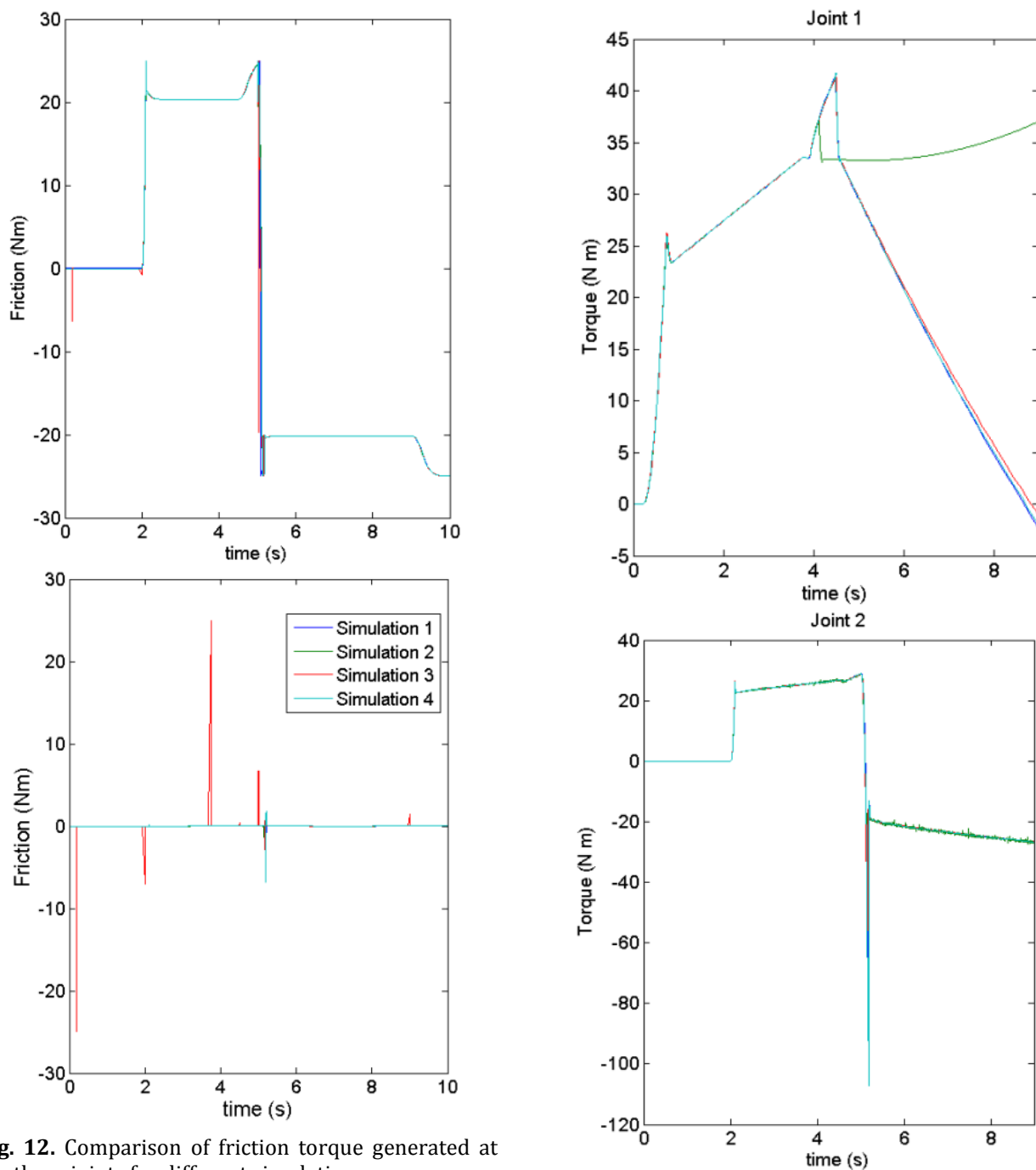

Fig. 11. Manipulator space in 3 dimensions.

Fig. 12. Comparison of friction torque generated at the three joints for different simulations.
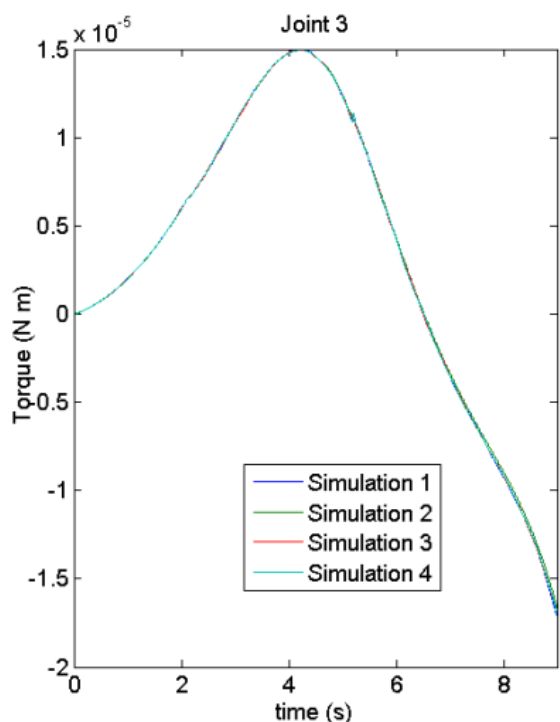
Fig. 13. Control torques from the controller for the three planar joints of the manipulator.
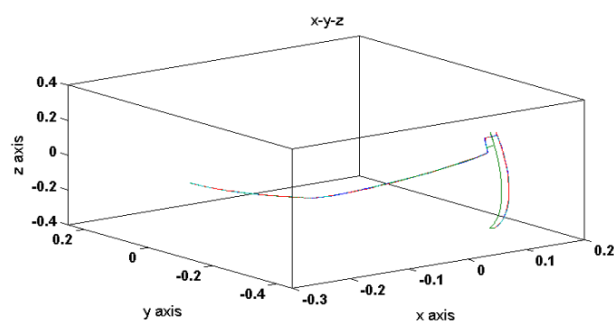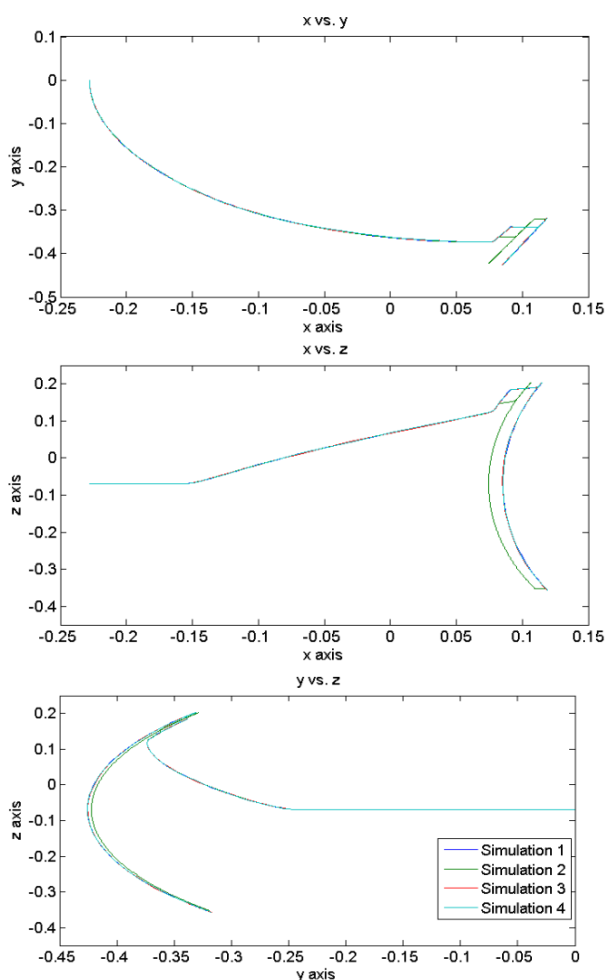

Fig. 14. Comparison of end effector motion in task manipulator task space for different simulations.
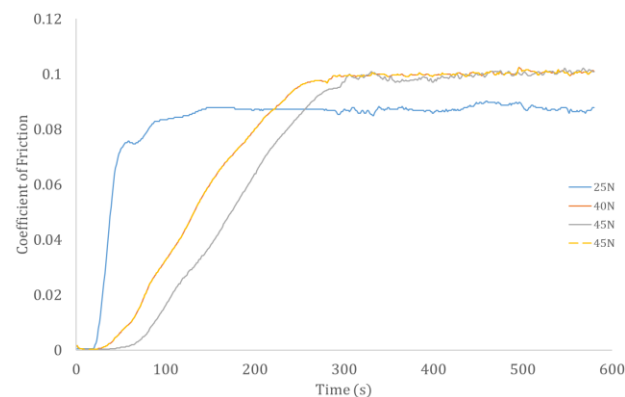

Fig. 15. Coefficient of friction measured by using micro-friction tribometer.

Comparison of the friction torques generated in joints gives an insight on the effect of the numerical solver on the solution. Stiff solvers have been selected where smaller step sizes are required. The difference in output parameters may be attributed to the solver step size. Simulations 1, 3 and 4 appear to agree. Simulation 3 takes minimum execution time. Therefore, solvers used in simulations 1, 3 and 4 may be suitable for simulation involving friction.

4.2. Coefficient of friction from micro-friction test

The coefficient of friction is measured by using reciprocating micro friction tribometer. It is observed that the value of friction was stabilised in 200-300 s into the test which was conducted for 10 minutes. The values of the coefficient of friction were observed to lie between 0.08 and 0.11 for the fully lubricated contact conditions. Therefore, low frictional torqueses are likely to be generated in newer machinery with close fit at the joints. However, with continued usage of mechanism, there is likely to be wear in the joint which will alter friction and affect the joint dynamics. The results from Bond graph simulation are presented in Fig. 15.

4.3. Bond graph Simulation

The objective of this research is to pick and place the fragile and soft objects without slippage by using a soft fingered gripper. 20Sim [65] was used for simulation of Bond graph model. In simulation, it was found that after gripping the object, the displacement due to its weight is considerably small, i.e., only in micrometres. Experimental results show that there is no slippage after gripping the object.

a)

b)

c)

Table 5. Simulation results from 20Sim [41].
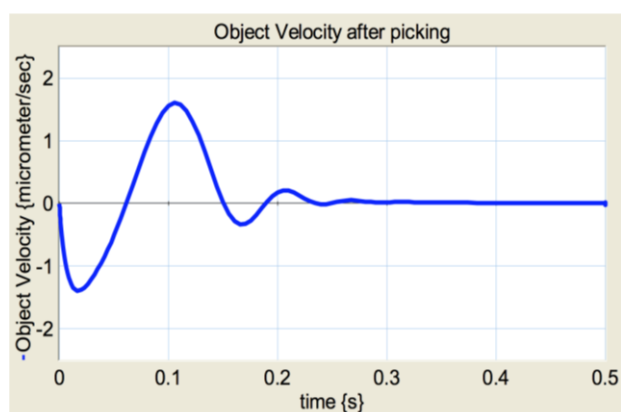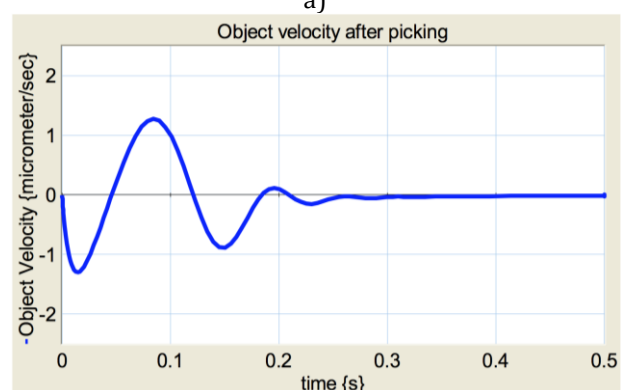
Fig. 16. a. Velocity of object during grasping at stiffness = 10 N/m, damping = 5ns/m and friction = 5 N.s/m, b. Velocity of object during grasping at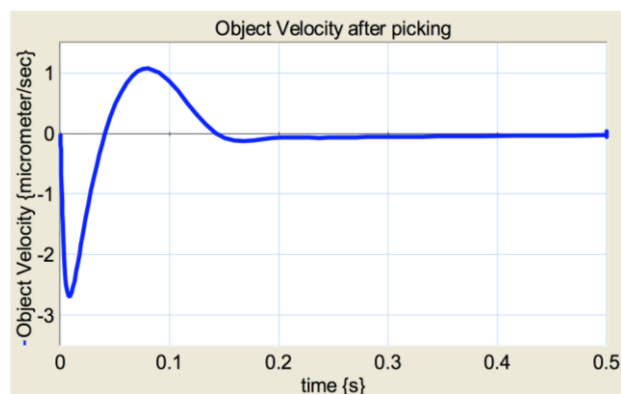 stiffness = 10 N/m, damping = 10 N.s/m and friction = 10 N.s/m, c. Velocity of object during grasping at stiffness = 20 N/m, damping = 20 N.s/m and friction = 20 N.s/m.

Simulations have been repeated for a range of stiffness and damping values to study the effect of these parameters on the friction and the system stability. The values of R_d and R_f in each soft finger were varied from 5 N.s/m to 20 N.s/m and that of K_s was varied from 10 to 20 N/m. The mass of the object was fixed at 100g for all simulations. Consolidated table containing all the simulated results are given in [41] (**Error! Reference source not found.**). The velocity of the object and its displacement for 1N force was observed. The velocity of the object after gripping has been shown in Fig. 16. The object slips initially during the grasping. Steady state value of zero displacement was achieved after 200 milliseconds.

5. CONCLUSIONS

This paper addresses two challenges. The first challenge is the rapid development of manipulator mechanics using high end virtual prototypes which is extended to include the effects of joint friction parameters. With the increase in computational resources, virtual prototyping has been increasingly used to model the mechanics of new designs, leading to both time and cost savings. In this work, it is demonstrated this by using computer aided drawing and multibody dynamics to develop the prototype of a humanoid manipulator. Additionally, the friction model has been incorporated into the joints of the robotic arm. The value of the coefficient of friction from tribo-tests has been used to run several simulations of the manipulator mechanics.

The second problem analysed in this paper deals with the issue of effective grasping of soft and fragile objects. Bond Graph method is used to model the end interactions of the viscoelastic grip on fragile objects. Simulation of the model demonstrates the stabilising effect of linear viscoelastic fingertips grasping fragile objects.

#	$K_{s1} = K_{s2} = K_{s3}$ [N/m]	$R_{d1} = R_{d2} = R_{d3}$ [N.s/m]	$R_{f1} = R_{f2} = R_{f3}$ [N.s/m]	Peak velocity [μm/s]			Settling Time for Steady State Velocity [s]			Peak Displacement [mm]			Steady State Value of Displacement [mm]		
				v_x	v_y	v_z	v_x	v_y	v_z	x	y	z	x	y	z
1	10	5	5	-1.2	-1.7	-1.4	0.4	0.5	0.4	-0.036	-0.12	-0.05	-0.025	-0.043	-0.032
2	10	10	10	-2.6	-2.8	-2.7	0.5	0.8	0.5	-0.6	-0.14	-0.08	-0.025	-0.043	-0.032
3	10	15	15	-4.0	-4.2	-4.1	0.3	1.0	0.6	-0.072	-0.14	-0.089	-0.028	-0.037	-0.032
4	10	20	10	-5.5	-5.5	-5.5	0.4	0.8	0.7	-0.08	-0.137	-0.09	-0.030	-0.037	-0.032
5	20	5	5	-1.3	-1.7	-1.4	0.6	0.8	0.6	-0.037	-0.126	-0.091	-0.032	-0.036	-0.033
6	20	10	10	-2.7	-2.9	-2.8	0.6	0.9	0.6	-0.06	-0.14	-0.08	-0.032	-0.036	-0.033
7	20	20	10	-5.5	-5.5	-5.5	0.4	0.8	0.6	-0.08	-0.137	-0.09	-0.032	-0.036	-0.033

Optimised values of damping and stiffness for stable grasp are determined from the experimentations. Soft fingertips and rotation mechanism have been designed. The property of viscoelasticity of material is used in fine tuning the grip at the fingertips. It has been concluded based on the results of simulation that by varying the values of parameters as stiffness, damping and friction at the contact interface, velocity of grasped object and displacement during grasping can be controlled. These parameters also influence the peak value of velocity and stability of the grasp and their variation can be used for performing in-grasp fine manipulation of the object. Successful experiments were performed by gripping, picking and placing two objects, a fragile egg and a soft tomato.

Acknowledgement

REFERENCES

[1] S. Ivaldi, V. Padois and F. Nori, "Tools for dynamics simulation of robots: a survey based on user feedback", *CoRR*, pp. 1-15, 2014.

[2] M. Dooner, J. Wang and A. Mouzakitis, "Dynamic modelling and experimental validation of an automotive windshield wiper system for hardware in the loop simulation", *Syst. Sci. Control Eng.*, vol. 3, no. 1, pp. 230–239, 2015.

[3] S.E. Tomlinson, R. Lewis and M.J. Carré, "The effect of normal force and roughness on friction in human finger contact", *Wear*, vol. 267, no. 5–8, pp. 1311–1318, 2009.

[4] N. Xydas and I. Kao, "Modeling of Contact Mechanics and Friction Limit Surfaces for Soft Fingers in Robotics, with Experimental Results", *Int. J. Rob. Res.*, vol. 18, no. 9, pp. 941–950, 1999.

[5] K.B. Shimoga and A.A. Goldenberg, "Soft materials for robotic fingers", *Robot. Autom. 1992. Proceedings., IEEE Int. Conf.*, vol. 2, pp. 1300–1305, 1992.

[6] A. Ghafoor, J.S. Dai and J. Duffy, "Fine motion control based on constraint criteria under pre-loading configurations", *J. Robot. Syst.*, vol. 17, no. 4, pp. 171–185, 2000.

[7] A. Ghafoor, J.S. Dai and J. Duffy, "Stiffness Modeling of the Soft-Finger Contact in Robotic Grasping", *J. Mech. Des.*, vol. 126, no. 4, pp. 646–656, 2004.

[8] J.S. Dai, D.R. Kerr and R. Group, "A six-component contact force measurement device based on the Stewart platform", *Proc. Inst. Mech. Eng. Part C J. Mech. Eng. Sci.*, vol. 214, no. 5, pp. 687–697, 2000.

[9] A. Khurshid, A. Ghafoor, M. A. Malik and M. Afzaal, "Robotic Grasping and Fine Manipulation Using Soft Fingertip", *Adv. Mechatronics*, pp. 155–174, 2011.

[10] V. Tincani *et al.*, "Implementation and control of the Velvet Fingers: A dexterous gripper with active surfaces", in: *2013 IEEE Int. Conf. Robot. Autom.*, pp. 2744–2750, May 2013.

[11] E. Brown *et al.*, "From the Cover: Universal robotic gripper based on the jamming of granular material", *Proc. Natl. Acad. Sci.*, vol. 107, no. 44, pp. 18809–18814, 2010.

[12] M. Popović *et al.*, "A strategy for grasping unknown objects based on co-planarity and colour information", *Rob. Auton. Syst.*, vol. 58, no. 5, pp. 551–565, 2010.

[13] V.N. Dubey and R.M. Crowder, "Grasping and control issues in adaptive end effectors", *Proc. DETC'04 ASME 2004 Des. Eng. Tech. Conf. Comput. Inf. Eng. Conf.*, pp. 1–9, 2004.

[14] L.U. Odhner *et al.*, "A compliant, underactuated

hand for robust manipulation", *Int. J. Rob. Res.*, vol. 33, no. 5, pp. 736–752, 2014.

[15] H.-J. Cha, K.C. Koh and B.-J. Yi, "Stiffness modeling of a soft finger", *Int. J. Control. Autom. Syst.*, vol. 12, no. 1, pp. 111–117, 2014.

[16] L. Biagiotti, F. Lotti, C. Melchiorri and G. Vassura, "How Far Is the Human Hand ? A Review on Anthropomorphic Robotic End-effectors Basic concepts", *Hand*, p. 1-21, 2004.

[17] K. Waldron, K. Waldron, J. Schmiedeler and J. Schmiedeler, "Kinematics", *Springer Handb. Robot.*, pp. 9–33, 2008.

[18] R. Featherstone and D.E. Orin, "Dynamics", *Robotics*, pp. 35–65, 2008.

[19] G.J. Monkman, S. Heute, R. Steinmann and H. Schunk, "Introduction to Prehension Technology", *Robot grippers*, pp. 1–18, 2007.

[20] P. Schneider and W. Servis, "Robot grippers in systems projects", *Ind. Robot An Int. J.*, vol. 15, no. 4, pp. 211–215, 1988.

[21] R. Alqasemi, S. Mahler and R. Dubey, "A Double Claw Robotic End-Effector Design", *Recent Advances in Robotics*, pp. 1–6, 2007.

[22] B.M. Jau, "Dexterous Telemanipulation with Four Fingered Hand System", *Robot. Autom. 1995. Proceedings., 1995 IEEE Int. Conf.*, vol. 1, pp. 338–343, 1995.

[23] D. Prattichizzo, M. Malvezzi and A. Bicchi, "On motion and force controllability of grasping hands with postural synergies", *IEEE Trans. Robot.*, vol. 2, no. 6, pp. 1–16, 2010.

[24] M.R. Tremblay and M.R. Cutkosky, "Estimating friction using incipient slip sensing during a manipulation task," in: *Proceedings IEEE International Conference on Robotics and Automation*, 1993, pp. 429–434.

[25] W.H. Ding, H. Deng, Q.M. Li and Y.M. Xia, "Control-orientated dynamic modeling of forging manipulators with multi-closed kinematic chains", *Robot. Comput. Integr. Manuf.*, vol. 30, no. 5, pp. 421–431, 2014.

[26] L.U. Odhner, R.R. Ma and A.M. Dollar, "Precision grasping and manipulation of small objects from flat surfaces using underactuated fingers", *Proceedings - IEEE International Conference on Robotics and Automation*, pp. 2830–2835, 2012.

[27] M.R. Cutkosky and P.K. Wright, "Friction, Stability and the Design of Robotic Fingers", *Int. J. Rob. Res.*, vol. 5, no. 4, pp. 20–37, 1986.

[28] S.E. Tomlinson, R. Lewis and M.J. Carré, "Review of the frictional properties of finger—object contact when gripping" *Proc. Inst. Mech. Eng. Part J J. Eng.*

Tribol., vol. 221, no. 8, pp. 841–850, 2007.

[29] M. Gabiccini, A. Bicchi, D. Prattichizzo and M. Malvezzi, "On the role of hand synergies in the optimal choice of grasping forces", *Auton. Robots*, vol. 31, no. 2–3, pp. 235–252, 2011.

[30] J. Aleotti and S. Caselli, "Part-based robot grasp planning from human demonstration", *Proc. - IEEE Int. Conf. Robot. Autom.*, pp. 4554–4560, 2011.

[31] D. Song, K. Huebner, V. Kyrki and D. Kragic, "Learning Task Constraints for Robot Grasping using Graphical Model – Bayesian Network", pp. 1579–1585, 2010.

[32] D. Berenson and S.S.S. Srinivasa, "Grasp synthesis in cluttered environments for dexterous hands," *2008 8th IEEE-RAS Int. Conf. Humanoid Robot. Humanoids 2008*, pp. 189–196, Dec. 2008.

[33] J.S. Son, E.A. Monteverde and R.D. Howe, "A tactile sensor for localizing transient events in manipulation", in: *Proceedings of the 1994 IEEE International Conference on Robotics and Automation*, 1994, pp. 471–476.

[34] M. H. Nazir, Z. Khan and K.R. Stokes, "Modelling of metal-coating delamination incorporating variable environmental parameters", *J. Adhes. Sci. Technol.*, vol. 29, no. 5, pp. 392–423, 2015.

[35] M.H. Nazir, Z.A. Khan and K.R. Stokes, "A holistic mathematical modelling and simulation for cathodic delamination mechanism – a novel and an efficient approach", *J. Adhes. Sci. Technol.*, vol. 29, no. 22, pp. 2475–2513, 2015.

[36] M.H. Nazir, Z.A. Khan and K.R. Stokes, "Optimisation of interface roughness and coating thickness to maximise coating–substrate adhesion – a failure prediction and reliability assessment modelling", *J. Adhes. Sci. Technol.*, vol. 29, no. 14, pp. 1415–1445, 2015.

[37] D. Keymeulen and C. Assad, "Investigation of the Harada Robot Hand For Space", *Jet Propuls. Lab.*, 2001.

[38] J.A. Bagnell *et al.*, "An integrated system for autonomous robotics manipulation", *2012 IEEE/RSJ Int. Conf. Intell. Robot. Syst.*, pp. 2955–2962, 2012.

[39] M.T. Mason, A. Rodriguez, S.S. Srinivasa and A.S. Vazquez, "Autonomous manipulation with a general-purpose simple hand", *Int. J. Rob. Res.*, vol. 31, no. 5, pp. 688–703, 2012.

[40] A. Khurshid, A. Ghafoor and M.A. Malik, "Modeling and Analysis of Soft Contact in Robotic Grasping Using Bond Graph Methods", *Adv. Mater. Res.*, vol. 189–193, pp. 1786–1792, 2011.

[41] A. Khurshid, A. Ghafoor, M.A. Malik and Y. Ayaz, "Modeling and analysis of robotic grasping using soft fingertips", in: *Proceedings CLAWAR2013*,

2013, pp. 642–650.

[42] J.C. Trinkle, "On the Stability and Instantaneous Velocity of Grasped Frictionless Objects", *IEEE Trans. Robot. Autom.*, vol. 8, no. 5, pp. 560–572, 1992.

[43] M. Salerno, K. Zhang, A. Menciassi and J. S. Dai, "A novel 4-DOFs origami enabled, SMA actuated, robotic end-effector for minimally invasive surgery", in: *2014 IEEE International Conference on Robotics and Automation (ICRA)*, 2014, pp. 2844–2849.

[44] S. Degeratu, P. Rotaru, S. Rizescu and N.G. Bîzdoacă, "Thermal study of a shape memory alloy (SMA) spring actuator designed to insure the motion of a barrier structure", *J. Therm. Anal. Calorim.*, vol. 111, no. 2, pp. 1255–1262, 2013.

[45] X. Zhang *et al.*, "Strong Carbon-Nanotube Fibers Spun from Long Carbon-Nanotube Arrays", *Small*, vol. 3, no. 2, pp. 244–248, 2007.

[46] C.S. Haines *et al.*, "Artificial muscles from fishing line and sewing thread", *Science*, vol. 343, no. 6173, pp. 868–872, 2014.

[47] J.M. Hollerbach, I.W. Hunter and J. Ballantyne, "A comparative analysis of actuator technologies for robotics", *Robot. Rev. 2*, 1991.

[48] E.T. Roche *et al.*, "A bioinspired soft actuated material", *Adv. Mater.*, vol. 26, no. 8, pp. 1200–1206, 2014.

[49] J.A. Lee, R.H. Baughman and S.J. Kim, "High performance electrochemical and electrothermal artificial muscles from twist-spun carbon nanotube yarn", *Nano Converg.*, vol. 2, no. 1, p. 8, 2015.

[50] A.J. Koivo, "Kinematics of Excavators (Backhoes) for Transferring Surface Material", *J. Aerosp. Eng.*, vol. 7, no. 1, pp. 17–32, 1994.

[51] B. Donald, "Forward Kinematics : The Denavit-Hartenberg convention".

[52] A.J. Koivo, M. Thoma, E. Kocaoglan and J. Andrade-Cetto, "Modeling and Control of Excavator Dynamics during Digging Operation", *Journal of Aerospace Engineering*, vol. 9, no. 1. pp. 10–18, 1996.

[53] B.P. Patel and J.M. Prajapati, "Dynamics of Mini Hydraulic Backhoe Excavator: A Lagrange-Euler (LE) Approach", *Int. J. Mech. Aerospace, Ind. Mechatron. Manuf. Eng.,* vol. 8, no. 1, pp. 202–211, 2014.

[54] S. Šalinić, G. Bošković and M. Nikolić, "Dynamic modelling of hydraulic excavator motion using Kane's equations", *Autom. Constr.*, vol. 44, pp. 56–62, Aug. 2014.

[55] N.K. Myshkin and A.Y. Grigoriev, "Roughness and texture concepts in tribology", *Tribology in Industry*, vol. 35, no. 2, pp. 97–103, 2013.

[56] The Mathworks Inc. UK, "Rotational Friction", *Mathworks Documentation*, 2015.

[57] C.S. Ramesh, S. Khan, K. Zulfiqar and K.S. Sridhar, "Slurry Erosive Wear Behavior of Hot Extruded Al6061-Si$_3$N$_4$ Composite", *Mater. Sci. Forum*, vol. 773–774, pp. 454–460, 2013.

[58] C.S. Ramesh, M.L. Shreeshail, G. Harsha and K. Zulfiqar, "Air Jet Erosion Wear Behavior of Al6061-SiC-Carbon Fibre Hybrid Composite", *Mater. Sci. Forum*, vol. 773–774, pp. 547–554, 2013.

[59] A. Khurshid and M.A. Malik, "Modeling and Simulation of an automotive system by using Bond Graphs," in: *10th International Symposium on Advanced Materials ISAM*, 2007.

[60] A. Khurshid and M.A. Malik, "Bond Graph Modeling and Simulation of Impact Dynamics of a Car Crash," in: *5th International Bhurban Conference On Applied Sciences And Technology IBCAST*, 2007.

[61] M.A. Malik and A. Khurshid, "Bond graph modeling and simulation of mechatronic systems", in: *7th International Multi Topic Conference, 2003. INMIC 2003.*, 2003, pp. 309–314.

[62] M.A. Chowdhury, D.M. Nuruzzaman, A.H. Mia, and M.L. Rahaman, "Friction coefficient of different material pairs under different normal loads and sliding velocities", *Tribology in Industry*, vol. 34, no. 1, pp. 18–23, 2012.

[63] M.A. Chowdhury, D.M. Nuruzzaman, B.K. Roy, S. Samad, R. Sarker and A.H.M. Rezwan, "Experimental Investigation of Friction Coefficient and Wear Rate of Composite Materials Sliding against smooth and rough mild steel counterfaces", *Tribology in Industy*, vol. 35, no. 4, pp. 286–296, 2013.

[64] J. Lakshmipathy and B. Kulendran, "Reciprocating wear behaviour of 7075Al/SiC and 6061Al/Al2O3 composites: A study of effect of reinforcement, stroke and load", *Tribology in Industry*, vol. 36, no. 2, pp. 117–126, 2014.

[65] University of Twente, "20sim", 2015.

Nomenclature

α_i	Angle between z axes of coordinate systems of two consecutive links
θ_{actual}	Output angular parameters from the model
$\theta_{desired}$	Desired input angle for simulation
θ_i	Joint rotation angles between links

$\dot{\theta}_i$	Angular velocity		position
		FK	Forward Kinematics
$\ddot{\theta}_i$	Angular acceleration	IK	Inverse Kinematics
τ_{brk}	Breakaway torque	G	Gravity Forces Matrix
$\tau_{br.thr}$	Threshold breakaway torque	H	Centripetal forces matrix
τ_C	Coulomb friction torque	K_s	Springs stiffness in each soft finger (N/m)
τ	Control torque	m	Arbitrary constant in the friction contact model
μ	Coefficient of Friction		
ω	Angular velocity	M_f	Mass of each finger (kg)
ω_{thr}	Threshold angular velocity	M_o	Mass of the object being grasped (kg)
A_{i-1}^{i}	Kinematic transformation matrix	N	Filter coefficient (PID controller), Normal force at contact
B	Friction Forces matrix		
c_v	Coefficient of viscous friction	ODE	Ordinary differential equation
c_{trans}	Coefficient of transition	p_i	Coordinates of ith frame
CAD	Computer Aided Design	PID	Proportional Integral Derivative Controller
D	Inertia Matrix	R_f	Friction at each soft finger contact (Ns/m)
DAE	Differential Algebraic Equations	R_d	Damping in each soft finger (Ns/m)
DOF	Degrees(s) of Freedom	S_{fi}	Force applied on i^{th} soft finger (N)
e	Error signal between control and actual	S_e	Weight of the object (N)